Equations (25) and (29) give the first-order $\rho_1 = \rho_1(T)$. Equations (15) and (27) become $\zeta(T,\rho_1) = \zeta(T)$ and $\psi(T,\rho_1) = \psi(T)$, respectively. Then Eq. (26) yields the first-order temperature distribution of

$$z = -\frac{1}{\dot{S}} \int_{T_0}^{T} \psi(T)dT \tag{30}$$

where T_0 is determined from Eq. (19) for erosion alone, and $T_0 = T_a$ for combined erosion and ablation.

To obtain higher-order approximations, an iterative procedure may be set up by using the first-order temperature to obtain a second-order density which in turn is used to obtain a second-order temperature, etc. However, such a procedure is more tedious than solving Eqs. (14) and (16) directly. Furthermore, the first-order solution is in general sufficiently accurate for engineering purposes. A comparison of the first-order solution and the exact solution is shown in Fig. 1 for a sample problem. It is seen that the two solutions yield nearly identical results. The figure also shows that higher erosion rate results in lower heat storage and less decomposition.

Limitations for Finite-Difference Methods

It is highly desirable to examine the limitations and magnitudes of error in employing finite-difference techniques to solve heat transfer problems with high surface recession rate. Consider the case of a noncharring material. Then the exact solution is given by Eq. (28) which, for $T_\infty = 0$, becomes

$$T/T_0 = e^{-\phi z} \tag{31}$$

where $\phi = \dot{S}/\alpha$ with α being the thermal diffusivity of the material.

A second-order finite-difference equation for quasi-steady state and constant properties can be given in the form[3]

$$(U_{i+2} - 2U_{i+1} + U_i)/h^2 + \phi[(U_{i+2} - U_i)/2h] = 0 \tag{32}$$

where U denotes a temperature obtained by finite-difference method, h is a space interval (Δz), and $i = z/h$. Equation (32) can be reduced to

$$U_{i+1} = [(1 - \phi h/2)/(1 + \phi h/2)]U_i \tag{33}$$

The solution is obviously unacceptable if $h \geq 2/\phi$. Comparison of Eq. (33) with the exact solution given by Eq. (31) shows the accumulated relative error at z (node i) to be

$$E_i \equiv \left|\frac{U_i}{T_i} - 1\right| = \left|\frac{U_0}{T_0}\left(\frac{1 - \phi h/2}{1 + \phi h/2}\right)^i e^{i\phi h} - 1\right| \tag{34}$$

The error increases monotonically with ϕh for all i. For example, even with $U_0 = T_0$, an error of 50% is developed after one step and it increases to 75% after two steps if $h > 1.65\ \alpha/\dot{S}$. It is important to note that this conclusion holds regardless of the heat flux.

Another limitation on the size of h is due to the starting value of U_0/T_0. To assess this error, let the boundary condition for unknown surface temperature be represented by a second-order numerical expression of the form

$$(3U_0 - 4U_1 + U_2)/2h = Q_s/k \tag{35}$$

where Q_s denotes the conduction heat flux at the surface. Eliminating U_1 and U_2 by using Eq. (33) and deducing $T_0 = Q_s/k\phi$ from Eq. (31), one obtains

$$E_0 = \left|\frac{U_0}{T_0} - 1\right| = \frac{\phi^2 h^2}{4(1 + \phi h)} \tag{36}$$

The magnitude of error in surface temperature is

$$|U_0 - T_0| = Q_s E_0/k\phi \tag{37}$$

Thus, while the relative error depends on ϕh only, the absolute error depends on $Q_s/k\phi$ and ϕh. The errors are given by Eqs. (34, 36, and 37). It should be pointed out that in the transient period, the errors will be greater than those indicated.

References

[1] Munson, T. R. and Spindler, R. J., "Transient Thermal Behavior of Decomposing Materials, Pt. I: General Theory and Application to Convective Heating," IAS Paper 62-30, presented at the IAS 30th Annual Meeting, New York, Jan. 22–24, 1962.

[2] Rohsenow, W. M. and Choi, H. Y., *Heat, Mass, and Momentum Transfer*, Prentice-Hall, Englewood Cliffs, N. J., 1961, pp. 122–124.

[3] Carslaw, H. S. and Jaeger, J. C., *Conduction of Heat in Solids*, 2nd ed., Oxford, 1959, Chapt. XVIII.

Attitude Control of a Sun-Pointing Spinning Spacecraft by Means of Solar Radiation Pressure

M. Chandler Crocker II*
American Science and Engineering Inc., Cambridge, Mass.

Nomenclature

α_1,α_2	=	solar absorptivities, of sides 1 and 2 main paddles
ϵ_1,ϵ_2	=	thermal emissivities, sides 1 and 2 of main paddles
α_s	=	solar absorptivity of the spin rate regulator paddles
H	=	solar constant = 1400 w/m^2
v	=	velocity of light = 3×10^8 m/sec
A,A_s	=	areas of main and spin regulator paddles
t	=	time, sec
d,d_s	=	distances from the center of mass of the satellite to the centers of pressure of the main paddle and the spin regulator paddles, respectively
I	=	moment of inertia of the satellite
ω,ω_0	=	spin rate and initial value, respectively
F_1,F_2,F_3	=	forces on a paddle due to reflected sunlight and thermal emission
L_r,L_θ,L_Φ	=	components of torque on the satellite in spherical coordinates due to the main paddles
$L_{rS},L_{\theta S},L_{\Phi S}$	=	components of torque on the satellite due to the spin regulator paddles
β	=	angle between plane of the spin regulator paddles and plane of the main paddles when $\gamma = 0$
γ	=	angle between spin regulator paddles and spin axis
θ,Φ	=	angular position of the spin axis on spherical coordinates with the sun along the Z axis
θ_0,Φ_0	=	initial values of θ and Φ

Introduction

SEVERAL authors[1–7] have considered using radiation pressure for attitude control of nonspinning spacecraft. Ule[8] was the first to describe a spinning satellite attitude control system for orienting the spin axis of a satellite so that the spin axis was coincident with the satellite-sun line by utilizing radiation pressure. Additional work has been done on similar devices.[9–13] Howland[14] et al. have devised a device for orienting the spin axis of a satellite perpendicular to the satellite-sun line by means of radiation pressure. This Note describes a method of maintaining the spin axis of a satellite pointing toward the sun. At the same time the spin of the satellite is maintained at a constant rate. The method requires no moving parts except springs. Electronic sensors are not required and the system requires no electrical power. As such it is well suited for satellites that are to have many years of operational life. Two larger main paddles parallel to the spin axis are used for spin axis pointing (Fig. 1); they

Received November 24, 1969.

* Senior Systems Engineer.

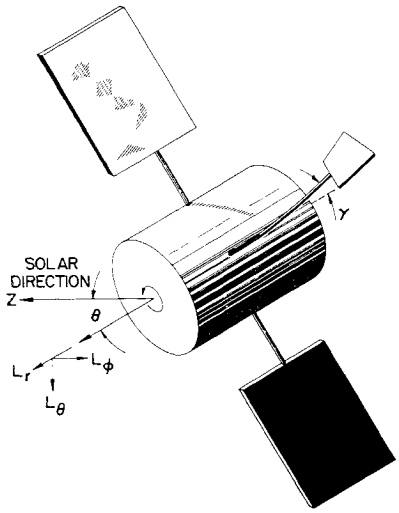

Fig. 1 Solar paddle arrangement.

have a high α on one surface and a low α on the other; $\alpha_2 \gg \alpha_1$, and $\epsilon_1 > \epsilon_2$. Two smaller paddles are mounted on springs and are set at an angle to the spin axis to provide a propeller torque. As spin rate increases, the smaller paddles swing out and the propeller torque action tends to decrease the spin rate. The main paddles, on the other hand, tend to increase the spin rate. The spin rate is maintained at a value where the net torque of the two sets of paddles is zero. Both sets of paddles set up torques that precess the spin axis so as to decrease θ.

Radiation Pressure Forces and Torques

There are basically three forces set up on a paddle when exposed to radiation pressure as shown in Fig. 2. One is due to the reflection of the plate and is normal to the plate

$$F_1 = (2 - \alpha_1)HAc^2\Psi/v$$

Another is along the plate:

$$F_2 = \alpha_1 HAs(2\Psi)/2v$$

The third is due to thermal emission from the plate

$$F_3 = 2\alpha_1(\epsilon_1 - \epsilon_2)HAc\Psi/3(\epsilon_1 + \epsilon_2)$$

where s $\equiv$ sin, c $\equiv$ cos, and it has been assured that there is no angular dependence of α and ϵ, and the paddle is thermally isolated from the satellite (it does not have to be). These forces, which act on the center of pressure of the paddles, are averaged over one revolution of the satellite. The resulting average torque is

$$L_r = HAd(\alpha_2 - \alpha_1)s^2\theta/4v + HAd(\alpha_1 - \alpha_2) \times (\epsilon_1 - \epsilon_2)s\theta/3\pi v(\epsilon_1 + \epsilon_2)$$

$$L_\theta = (\alpha_1 - \alpha_2)HAds(2\theta)/8v$$

$$L_\Phi = (3\alpha_2 + \alpha_1 - 4)HAds^2\theta/3\pi v$$

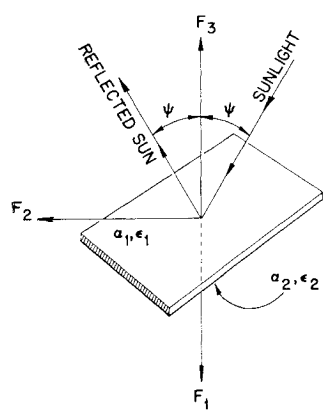

Fig. 2 Forces acting on a paddle.

The torque from the spin regulator panels is

$$L_{rs} = -HA_sd_s(2 - \alpha_s)s\gamma s\beta[c^2\theta c^2\beta s^2\gamma + s^2\theta(c^2\beta c^2\gamma/2 + s^2\beta/2)]$$

$$L_{\theta s} = -HA_sd_s(2 - \alpha_s)s^2\theta s^2\beta c\beta s^3\gamma/4v$$

$$L_{\Phi s} = -HA_sd_s(2 - \alpha_s)s^2\theta s^2\gamma c\beta/4v$$

Here γ becomes larger as the speed of the satellite increases due to the action of centrifical force on the smaller speed-regulator paddles that are maintained on leaf springs.

Satellite Dynamics

If we assume that a) no other torques such as gravity gradient torques act on the satellite, b) an adequate nutation damper is mounted in the spacecraft such that the angular momentum vector is very close to the spin axis direction, c) the sun does not move in inertial space during acquisition, and d) the effects of the spin regulator paddles may be neglected during acquisition, then the motion of the spin axis may be expressed in closed form during the time of acquisition. The time of acquisition is the period of time after the spacecraft is put in orbit with some initial value of $\theta_0 < 90°$. The equations of motion are

$$\tan(\theta/2) \approx \tan(\theta_0/2)\exp[(\alpha_1 - \alpha_2)HAdtc\theta_0/4vI\omega_0]$$

$$\omega = 4\omega_0(\alpha_1 + \alpha_2)(\epsilon_1 - \epsilon_2)c\theta\tan(\theta_0/2 + \pi/4)/3\pi(\alpha_2 - \alpha_1)(\epsilon_1 + \epsilon_2)\cdot c\theta_0\tan(\theta/2 + \pi/4)$$

$$\Phi = \Phi_0 + 4(3\alpha_2 + \alpha_1 - 4)\ln[\tan(\theta/2 + \pi/4)/\tan(\theta_0/2 + \pi/4)]/3\pi(\alpha_2 - \alpha_1)$$

The time to reduce an initial $\theta_0 = 60°$ to $\theta = 5°$ for a satellite with $\alpha_2 = 0.9$, $\alpha_1 = 0.04$, $A = 1$ m^2, $I = 0.2$ kg m^2, $\omega_0 = 0.1$, $\epsilon_1 = 0.8$, $\epsilon_2 = 0.72$, and $d = 2$ m is $t = 15$ days. A computer simulation was done to include the motion of the sun about the spin axis in inertial space, and the foregoing closed-form solution gave a good approximation to the computed "actual" motion of the spin axis.

A simulation was also done to take into account the action of the spin regulation panels. The spring action was assumed to be such that $\gamma = 45°$ for $\omega \geqq 0.1$ and $\gamma = 0°$ for $\omega \leqq 0.05$. For values of $A_s = 0.1$, $\beta = 35°$, $d_s = 1$ m and $A_s = 0.04$, it was found that the spin axis would track the sun such that the spin axis was maintained to within 0.75° of the solar direction.

References

[1] Acord, J. D. and Nicklas, J. C., "Theoretical and Practical Pressure Attitude Control for Interplanetary Spacecraft," AIAA Paper 63-327, Cambridge, Mass., 1963.

[2] Frye, W. E. and Stearns, E. V. B., "Stabilization and Attitude Control of Space Vehicles," *ARS Journal*, Vol. 29, 1959, pp. 927–931.

[3] Hilbard, R. R., "Attitude Stabilization Using Focused Radiation Pressure," *ARS Journal*, Vol. 31, 1961, pp. 844–845.

[4] Sohn, R. L., "Attitude Stabilization by Means of Solar Radiation Pressure," *ARS Journal*, Vol. 29, 1959, pp. 371–373.

[5] Hegstrom, R. J., "Satellite Attitude Stabilization by Means of Solar Sail," AS-442-382, Jan. 1964, Purdue Univ., Lafayette, Ind.

[6] Schalkowsky, S., "Attitude Control by Radiation Pressure," TIS-61SD77, May 1961, General Electric Co.

[7] Merrick, V. K., Moran, F. J., and Tinling, B. E., "A Technique for Passive Attitude Control of Solar Oriented Interplanetary Spacecraft," TN D-4641, July 1968, NASA.

[8] Ule, L. A., "Orientation of Spinning Satellites by Radiation Pressure," *AIAA Journal*, Vol. 1, No. 7, July 1963, pp. 1575–1578.

[9] Carrol, R. and Linburg, R., "Dynamics of a Solar Pressure Stabilized Satellite," T-65-1, June 1965, Massachuetts Institute of Technology Center for Space Research.

[10] Peterson, C. A., "Use of Thermal Re-Radiative Effects in Spacecraft Attitude Control," CSRT-66-3, May 1966, Massachusetts Institute of Technology Center for Space Research.

[11] Colombo, G., "Passive Stabilization of a Sunblazer Probe by Means of Radiation Pressure Torque," CSR TR-66-5, 1966, Massachusetts Institute of Technology Center for Space Research.

[12] Harrington, J. C., "The Dynamics of a Spinning-Solar Pressure-Stabilized Satellite with Precession Damping." CSR-TR-66-6, June 1966, Massachusetts Institute of Technology Center for Space Research.

[13] Falcovitz, J., "Attitude Control of a Spinning Sun-Orbiting Spacecraft by Means of a Grated Solar Sail," CSR-TR-66-17, Dec. 1966, Massachusetts Institute of Technology Center for Space Research.

[14] Howland, B., Moriarty, B., and Wiesner, S. J., private communications, July 1964, Massachusetts Institute of Technology Lincoln Lab.

Copolymer of Styrene and Oxygen as Potential Rocket Fuel

R. P. Rastogi,* K. Kishore,† and B. K. Chaturvedi‡
Chemistry Department, University of Gorakhpur, Gorakhpur U.P., India

VERY little attention has been paid to the use of oxygen copolymers (peroxidic polymers) as hybrid fuels or in solid composite propellants as fuel binders. This Note describes preparation of oxygen copolymers with styrene and presents strand burning rate data for composite propellants using them with ammonium perchlorate.

Experimental

The copolymers were prepared from styrene (Bareilly Synthetic Rubber Ltd.), commercial grade oxygen and benzoyl peroxide as follows.[1] Oxygen was then passed slowly into 200 g of styrene at 50°C for 10 to 60 min, then 2 g of benzoyl peroxide was added, and the mixture was kept on a water bath for 3–5 hr. When it became sufficiently viscous, it was poured into molds and cured at 70–80°C for 2–3 days. The following reaction is supposed to take place,

$$H_2C = CH \cdot C_6H_5 + O_2 \rightarrow \left(CH_2-\underset{\displaystyle C_6H_5}{\underset{|}{CH}}-O-O\right)_n$$

Molecular weight could be varied by passing oxygen for different time intervals.

Table 1 Burning rates of polymer/ammonium perchlorate solid propellants at 30°C, 1 atm

% AP by weight	r_b, cm/sec: Polystyrene propellant	r_b, cm/sec: Copolymer[a] propellant
65	0.046	0.047
70	0.086	0.113
75	0.093	0.160
80	0.118	0.280

[a] Oxygen was passed for 60 min at 50°C for preparing the polymer.

Received September 26, 1969; revision received December 10, 1969. Thanks are due to Kilachand Devchand and Co., Pvt. Ltd., for the gift of Styrene.

* Professor of Chemistry.
† Lecturer in Chemistry.
‡ Ph.D. Scholar.

Table 2 Comparison of propellant properties

Polymer[a]	Hardness R_b scale	Load to deform, tons	Mass burning rate, $\dot{m}$, g/sec
Polystyrene	55	3.5	0.111
Oxygen copolymer-I	43	2.5	0.106
Oxygen copolymer-II	40	2.0	0.094

[a] In the preparation of copolymers I and II oxygen was passed for 15 and 20 min at 50°C, respectively.

The densities of the polymer samples were determined by Nichalson's hydrometer. The weight average molecular weight M_w was determined by viscosity method by using the following empirical relationship,

$$[\eta] = 1.03 \times 10^{-4} M_w^{0.74} \quad (1)$$

where the constants, 1.03×10^{-4} and 0.74 refer to the polystyrene-benzene system, and $[\eta]$ is the intrinsic viscosity. The molecular weights so determined are only rough estimates because the constants would also depend on the nature of the polymer. The molecular weights are found to be of the order of 10^5.

Solid-propellant strands were prepared by mixing powdered ammonium perchlorate (AP) which was obtained from Central Electro-Chemical Laboratories, Karaikudi, with the viscous resin in a mortar and curing in molds for 10–15 days. Then a coating of inhibiter was applied to prevent burning down the side, and the strands, kept in vertical position, were ignited from the top. The linear burning rate (r_b) results are given in Table 1.

To simulate hybrid rocket operation with a copolymer fuel, center-perforated, cylindrical grains, 3.8 cm long with a port diameter of 0.5 cm, were made. Oxygen was passed through the grain at 12 liter/min. The grain was then ignited and the change in diameter with oxygen flow time t was noted. This was used to calculate the mass burning rate,

$$\dot{m} = \pi\rho l(r_2^2 - r_1^2)/t \quad (2)$$

where ρ and l are the density and length of the polymer sample, and r_1 and r_2 are the initial and final port radii. Propellant hardnesses were determined with a Rockwell hardness testing machine using a $\frac{1}{16}$-in. ball diameter and a 100-kg load on the Rb scale. Elastic deformability was measured on a high-pressure testing machine; the minimum weight in tons at which the sample (diameter, 2.02 cm; length, 6.61 cm) began to deform was noted. The results are given in Table 2.

For thermal degradation studies copolymer samples of ≈0.3 g were weighed and introduced in a preweighed test tube. The test tube was kept in a muffle furnace a fixed temperature for a definite time. The results computed from the weight losses (as described later) are given in the Table 3. The gaseous degradation products were analyzed by passing them through water and absolute alcohol. From the conventional organic analysis formaldehyde was identified in the aqueous solution, whereas benzaldehyde and styrene monomer were detected in the alcoholic solution.

Table 3 Thermal degradation results

Polymer[a]	Density, g/cm³	$k \times 10^5$: 230°C	$k \times 10^5$: 350°C	Energy of activation of thermal degradation, kcal/mole
Polystyrene	1.05	0.44	5.0	16
Copolymer-A	1.06	0.74	5.4	13
Copolymer-B	1.09	1.01	5.9	12
Copolymer-C	1.10	1.39	6.8	11

[a] In the preparation of copolymer-A, copolymer-B, and copolymer-C oxygen was passed for 10, 25, and 60 min, respectively, at 50°C.